A synoptic view of in-flight calibration plans of modern X-ray observatories[1]

Matteo Guainazzi[a,b], Laurence David[c], Catherine E. Grant[d], Eric Miller[d], Lorenzo Natalucci[e], Jukka Nevalainen[f], Robert Petre[g], Marc Audard[h]

[a]ESA-European Space Astronomy Centre (ESAC), Villafranca del Castillo, E-28692, Madrid, Spain
[b]Institute of Space and Astronautical Science, Japan Aerospace Exploration Agency (JAXA), 3-1-1 Yoshinodai, Chuo-ku, Sagamihara, Kanagawa 252-5210, Japan
[c]Harvard-Smithsonian Center for Astrophysics, 60 Garden St., Cambridge, MA 02138, USA
[d]Kavli Institute for Astrophysics and Space Research, Massachusetts Institute of Technology, 77 Massachusetts Ave., Cambridge, MA 02139-4307
[e]Istituto Nazionale di Astrofisica, INAF-IAPS, via del Fosso del Cavaliere, I-00133 Roma, Italy
[f]Tartu Observatory, 61602 Toravere, Estonia
[g]NASA, Goddard Space Flight Center, Greenbelt, MD, 20771 USA
[h]Department of Astronomy, University of Geneva, Ch. d'Ecogia 16, 1290, Versoix, Switzerland

Abstract. Ground-breaking observational scientific discoveries require adequate knowledge of the instrument performance. Ideally a complete set of ground-based calibration measurements should under-pin a full characterization of the physical model describing detectors flown on-board space observatory. More often than not, however, this is not the case due to time and budgetary restrictions during the development phase, or to the - somewhat inevitable and unpredictable - degradation of instrument performance in space. Furthermore, flight contingencies are often hard to reproduce on ground. In this paper we present a synoptic view of the set of celestial sources used for in-flight calibration of X-ray detectors by past and operational missions. This summary could be beneficial for future missions to optimize the critical early phases of their science operations.

Keywords: X-ray instrumentation - Operations - X-Rays:general.

Address all correspondence to: Matteo Guainazzi; E-mail: Matteo.Guainazzi@sciops.esa.int

1 The art of calibrating X-ray instruments

Ideally, calibration of space X-ray instruments is the result of a complete physical model supported by an adequate set of ground-based measurements under controlled conditions. Regrettably, time and budget pressure during the mission development phase, as well as the degradation of the instrument performance in space (radiation damage, contamination, electronic failures, degrading thermal environment) more often than not require re-calibration using celestial sources. "In-flight" calibration programs have been playing a crucial role in our understanding of the instrument scientific performance, as well as (and, often, more crucially) of their time evolution.

[1]This paper was written in the framework of the activities of the IACHEC Heritage Working Group

While X-ray astronomy is nowadays a fully mature and globally integrated science, calibration of X-ray space instruments was carried out for decades in isolation, and with little cross-talk among calibration teams of different instruments or little know-how transfer from older to newer mission (besides the natural transfer of calibration scientists to newer projects). This has led to a wide variety of approaches in dealing with similar calibration issues over different missions, as well as to a surprisingly large variety of celestial sources being used for the same calibration purpose. Moreover, the suitability of a celestial source for calibration purposes depends on the commensurability between observables related to the intrinsic astrophysical properties and instrument performance. For instance, thermal or velocity broadening of emission line profiles have a negligible impact on the calibration or energy scale and line spread function at CCD resolution ($\Delta E/E \sim 10$), while they must be taken into account at grating or calorimeter resolution ($\Delta E/E \gtrsim 100$).

The birth of the *International Astronomical Consortium for High-Energy Calibration* (IACHEC; `http://web.mit.edu/iachec/`)[1] in 2006 tried to alleviate this original sin, by achieving a better integration among calibration activities of operational high-energy observatories. In this context the IACHEC aims to provide standards for high energy calibration and coordinate cross calibration between different missions. This goal is reached through working groups, where IACHEC members cooperate to define calibration standards and procedures. The scope of these groups is primarily a practical one: a set of data and results (eventually published in refereed journals) will be the outcome of a coordinated and standardized analysis of reference sources ("high-energy standard candles"). Past, present and future high-energy missions can then use these results as a calibration reference. In this context one of the goals of IACHEC is to develop a web-based archive of calibrated data sets, spectral models, and response files for all "standard candles" from all high energy missions. This suite of calibrated data sets can then be used to ensure a proper

cross-calibration. Imprinted in the genetic code of the IACHEC is also the goal of providing future missions with a test-bed of consolidated experiences and good practices, that can be beneficial in designing and optimizing in-flight calibration plans.

Regrettably, calibration of X-ray astronomy instrumentation cannot rely on "standard candles" *stricto sensu*, *i.e.*, on sources whose absolute flux and spectrum is known once other astrophysical observables are measured. One must be content with sources for which an educated guess of the physical process responsible for their X-ray emission is available. These "X-ray standard candles" exhibit non-thermal broad-band spectra, or thermal spectra in the soft X-ray band ($\lesssim$2 keV). For each source in this set of "X-ray standard candles" the IACHEC aims to define data reduction and analysis procedures, and a reference astrophysical model; and to publish these, ideally in refereed journals.

In this paper we review the in-flight calibration plans of all the missions active in the IACHEC context (basically, all the operational X-ray observatories from the 90s of the past century to now). Our primary goal is providing a synoptic view of in-flight calibration programs of past and operational X-ray space missions that might be used by future missions to optimize the preparation of their calibration operations after launch.

X-ray astronomy is significantly older (and wiser) than the arbitrary time threshold applied to the missions covered by this paper. Reconstructing the quality and the accuracy of calibration measurements for older missions is often hard. Their data have not always been adequately preserved. While old archival data still contain excellent, and partly still uncovered science, we decided to discuss in this paper only those past and operational missions, whose calibration results have been discussed, and by a certain extent "validated" through the common work at the IACHEC. This choice introduces an historical bias in our synopsis, of which we, the authors, are well aware.

In this paper, we present the primary calibration sources used for the in-flight calibration of the following items: "high-resolution" Line Spread Function (LSF) and wavelength scale in § 2; redistribution, resolution and energy scale in X-ray CCDs in § 3; effective area in § 4 and § 5; Point Spread Function (PSF) in § 6; accuracy of event time assignment in § 7; and instrumental cross-calibration in § 8. In Appendix A we list the instruments discussed in this paper. The in-flight calibration and cross-calibration of NuSTAR is extensively discussed by Madsen et al. (2015).[2]

2 High-resolution LSF and wavelength scale

Spectra of X-ray bright cool stars have been used for the calibration of the Line Spread Function[†] and wavelength scale in the *Chandra*/LETG and HETG and the XMM-Newton/RGS (Tab. 1): ABDor, Algol, Capella, HR1099, and Procyon[3] (Fig. 1). Capella is on the average the brightest,

Table 1 Main sources used for the calibration of the LSF and wavelength scale in high-resolution detectors

Source	LETG	HETG	RGS
Capella	X	X	X
HR1099		X	X
Procyon	X		X

and the least variable in this sample: its historical RGS light curve exhibits a dynamical range of $\pm 15\%$ (Andy Pollock, private communication). ABDor and HR1099 exhibit large flaring activities, with flux changes of up to one order of magnitude on time scales as short as a few hours.[4,5]

The spectrum of some of these stars (Capella, most notably) is too soft to cover adequately the whole X-ray spectral bandpass. This is particularly important for the future calibration of the micro-calorimeter on-board ASTRO-H (Soft X-ray Spectrometer, SXS[6]) at the astrophysically cru-

[†]the *Line Spread Function* is the response to a monochromatic emission line in energy/wavelength space.

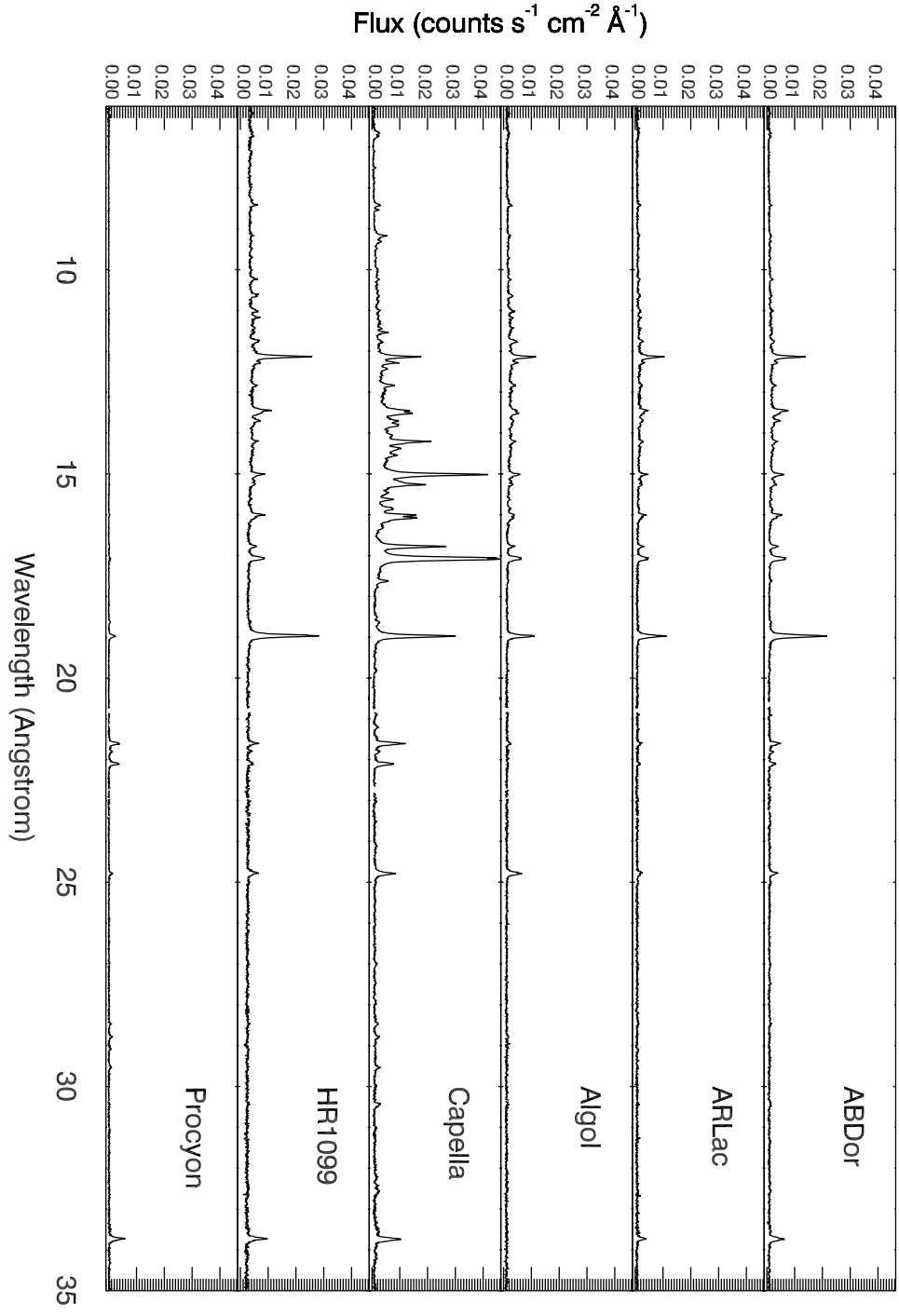

Fig 1 RGS spectra from the longest XMM-Newton observation of six cool stars used for the calibration of the LSF and wavelength scale. The spectra are displayed in on the same y-axis linear scale to ease comparison.

cial iron atomic transitions at 6–7 keV. HR1099 and ABDor are sufficiently hot for this purpose, but the thermal broadening of emission lines must be taken into account, potentially complicating the measurement of the instrumental properties. Alternatively, Fe-K fluorescence lines are commonly observed, for instance, in the spectra of X-ray Binaries (XRB). In particular, there exists population of heavily obscured XRBs, whose Fe line exhibits a very large (keV) Equivalent Width (EW). Among the best-studied (and brightest) examples of this sample are IGRJ16318-4848[7] and GX301-2.[8] Their lines are unresolved at the Chandra/HETG resolution. However, curve-of-growth analysis and other considerations are compatible with these lines being produced in the wind of the OB companion.[9] The Chandra upper limit on the width is 770 km/s, while the value stemming from terminal velocity of the star wind is 850 km/s. More worryingly, lines produced in stellar wind may have a complex structure, with red wings.[10] For these reasons it is therefore unclear yet of these sources could be used for the calibration of LSF and energy scale in detector with a eV-like resolution.

3 CCD redistribution, resolution and energy scale

The operation of X-ray Charge Coupled Devices (CCDs) differs from those in softer wave-bands in that each detected X-ray photon produces a charge cloud related to the energy of the photon. These charge packets are collected over some short integration time before being read out and processed into events by the instrument electronics. Ideally the amount of charge in each packet would be directly proportional to the incoming photon energy with a small dispersion (the spectral resolution), but in practice several processes can redistribute events to measured energies well away from the expectation. Some of these processes are related to the photon-CCD interaction (Si escape and fluorescence peaks, constant low-energy shelves from charge lost in non-interacting

substrate, and pile-up from multiple X-rays landing in the same region of the CCD); some are caused by the transfer of charge unique to CCDs (charge transfer efficiency, or CTI); and some are caused by the electronic read-out (gain drift). This energy redistribution, along with the efficiency of the telescope, filters, and detectors themselves, produce what is referred to as the ”response” of an X-ray instrument to a photon of a given energy.[‡]

While the redistribution shape can be in principle adequately characterized by illuminating the cameras with monochromatic beams on the ground, various forms of radiation damage in orbit produce spectral degradation. The resultant increase in CTI has required a re-calibration of the photon redistribution alongside the energy scale (or gain) in several space X-ray CCDs. Characterization of the CTI requires uniform illumination of the whole CCD with a source of known spectrum, ideally with well isolated (at CCD resolution) atomic transitions. In the XMM-Newton/EPIC cameras a specific position of the filter wheel (`CAL_CLOSED`) allows a ^{55}Fe source to illuminate the whole field-of-view. Similarly, a ^{55}Fe source illuminates the ACIS field-of-view when it is transferred into the stowed position before and after each passage through the radiation belts. The Suzaku/XIS and the Swift/XRT also make use of ^{55}Fe calibration sources which permanently illuminate small regions of the CCDs, however these are only sufficient to verify CTI corrections or monitor changes, not to properly measure the CTI across the detector. In addition, the ^{55}Fe source has a half-life time of only 2.7 years, a potential issue for long-lasting missions such as Chandra or XMM-Newton. The decreasing source flux, the different illumination conditions when compared with typical astronomical background, the limited spectral range where the ^{55}Fe produces atomic transitions, and the lack of field-filling calibration sources in some missions complicates CTI measurements using

[‡]A full description of the operation of an X-ray CCD is beyond the scope of this work, and the reader is referred to Chapter 3 of the “Handbook of X-ray Astronomy”.[11]

Table 2 Main sources used for the calibration of CTI, gain, and redistribution in CCD X-ray detectors

Source	ACIS	EPIC-MOS	EPIC-pn	XIS	XRT
1E0102-72	X	X	X	X	X
3C273		X			X
CasA	X	X	X		X
Cygnus Loop				X	
Perseus Cluster		X		X	
PKS2155-304		X			X
RXJ1856.5-3754		X			X
Tycho SNR		X	X		X
Vela SNR			X		
ζPuppis		X	X		
ζOrionis		X	X		

on-board sources alone.

These limitations require complementary observations of extended celestial sources with strong and well isolated (at CCD resolution) atomic transitions. A list of the main targets used for this purpose is given in Tab. 2.

The Vela Supernova Remnant (SNR) covers the whole $\simeq$30' side EPIC field-of-view, and it has been extensively used by the EPIC calibration team to calibrate the readout losses. Bright galaxy clusters such as Centaurus or Perseus have corroborated the calibration results.[12] The *Suzaku*/XIS and the Swift/XRT also make use of ^{55}Fe calibration sources which permanently illuminate small regions of the CCDs. Large scale sources such as the Cygnus Loop ($\simeq$3°), Puppis A (50'$\times$60'), Perseus Cluster ($\sim$1°) or the diffuse emission surrounding the Galactic Center have been used by *Suzaku*/XIS for CTI measurements. The characterization of transfer losses in the central area of the Swift/XRT made use of compact X-ray bright SNR such as Cas A, IC443, or Tycho. Tycho is also one of the targets used to characterize transfer losses in the EPIC-MOS. A compilation of

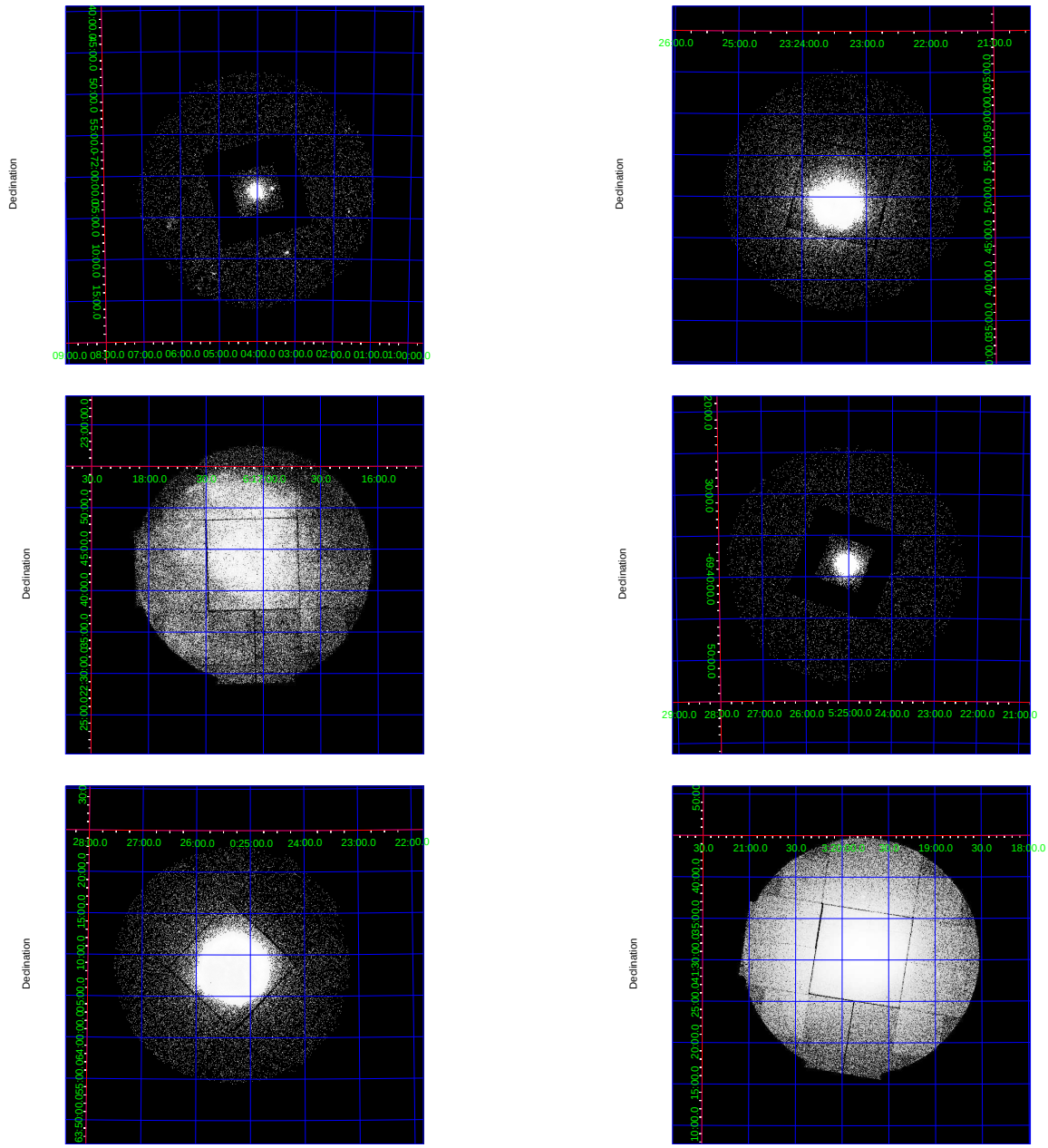

Fig 2 EPIC-MOS2 image of the deepest XMM-Newton observation of five SNR and one galaxy cluster used for calibration of the energy scale and redistribution in X-ray astronomy CCD detectors. *From top left to bottom right*, 1E0102-72, CasA, IC443, N132, Tycho, and the Perseus galaxy cluster. The size of the EPIC-MOS field of view is about 30'×30'.

EPIC-MOS images of SNRs is shown in Fig. 2 showing examples of compact (<2'), intermediate (≃5'), and large (≳30') sources used for calibration purposes. The corresponding EPIC-MOS count spectra in the 0.3–10 keV energy band are shown in Fig. 3.

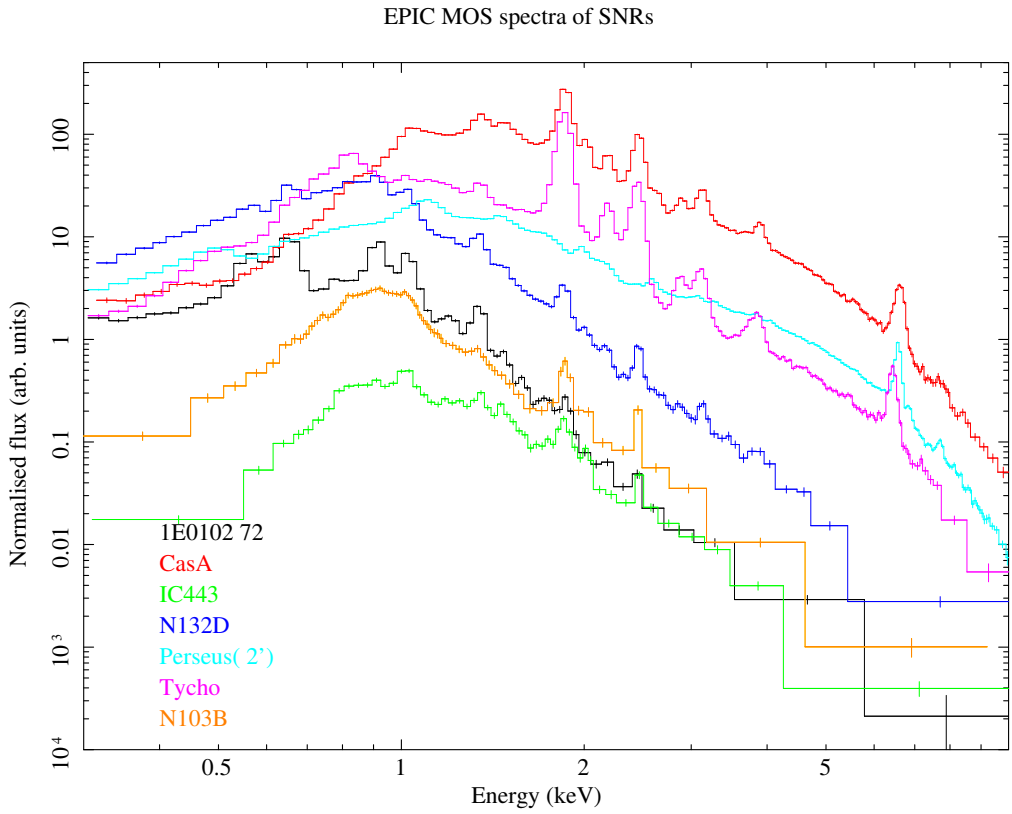

Fig 3 EPIC-MOS1 spectra of SNR and galaxy clusters used for CCD redistribution calibration

The study of spectral degradation in space also requires bright sources with well isolated (at CCD resolution) atomic transitions. A sample of these targets is also listed in Tab. 2. Cassiopeia A was the official first-light target for Chandra, primarily because it is bright, has many well-separated spectral features, and is matched in size to an ACIS CCD. However, it is also absorbed below 1 keV, *i.e.* close to the peak of the telescope effective area. The most used and studied source in the IACHEC context is, however, the compact ($\simeq$1' diameter) SNR 1E0102-72.3.[13] The combination of symmetric morphology, lack of Fe-L lines, strong and well isolated OVII, OVII, NeIX, and NeX emission lines, detailed empirical and astrophysical modeling, and deep available observations with all major operational CCD in space (together with a flux constant at a level of better than 1% in all knots; Plucinsky et al, in preparation) make of 1E0102-72.3 a widely

used "standard candle" in soft X-ray astronomy.[14] Stars like ζPuppis and ζOrionis offer alternatively strong NV lines. Very soft continuum sources such as the isolated neutron star RXJ1856.6-3754 offer complementary information thanks to their simple blackbody-like spectrum,[15] and - at least for the latter source - extreme stability.[16] Additional calibration of the redistribution can be achieved by looking at the agreement between data and models in bright power-law sources at energy ranges where the effective area exhibits the steepest gradients. Galactic black hole binaries such as LMCX-3, or radio-loud AGN such as 3C273 (Madsen et al., in preparation) and PKS2155-304[17] have been used for this purpose. These same sources have also been used by ACIS to calibrate the energy scale at low energies ($\lesssim$500 eV) using gratings observations.

Finally, it is possible to use heavily obscured sources to constrain the redistribution shelves. This is a particularly promising approach for CCD "Fast Modes" (EPIC-pn Timing and Burst Mode, XRT Window Timing Mode, or the Continuous Clocking Mode in ACIS). Bright obscured X-ray Binaries (XRBs) can in principle provide an almost uncontaminated view of photons redistributed below 2 keV. The main astrophysical issue to calibrate redistribution with obscured XRBs is disentangling the dust-halo scattering, or the coronal emission. We illustrate this issue with the bursting source Swift 1749.4-2807 observed with the EPIC-pn in *Timing Mode*. In this mode the CCD is read out continuously, integrating the charge of 10 pixels in the so-called "macro-pixels" and "sacrificing" the spatial information along the read-out direction. This mode is characterized by a much faster readout time than the standard imaging modes, and therefore allows the observation of sources up to a count rate of about about one third of the Crab Nebula avoiding coincidence losses of X-ray events (pile-up, X-ray loading) or optical and X-ray events (optical loading) in the same pixel within an integration frame time. Observations of X-ray obscured (column density $\gtrsim 10^{22}$ cm^{-2}) XRBs in EPIC-pn Timing Mode often exhibit a "soft excess" below the extrapola-

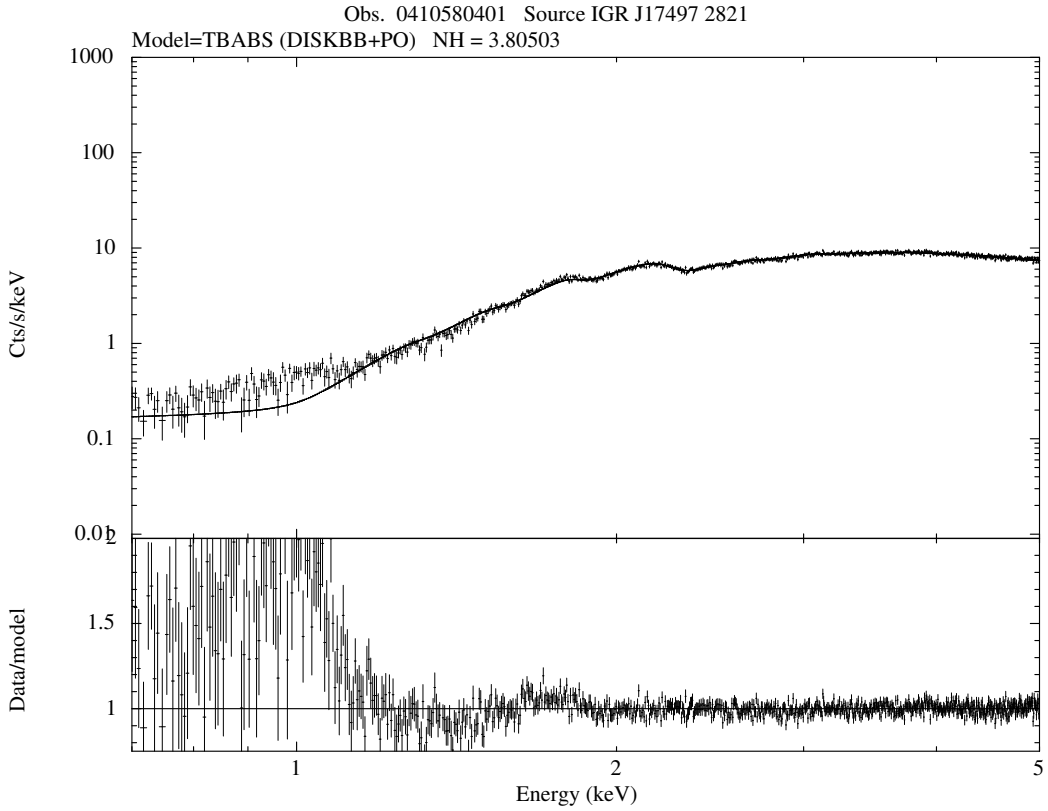

Fig 4 EPIC-pn Timing Mode time-averaged spectrum (*upper panel*) and residuals in units of data model ratio (*lower panel*) of the burster Swift 1749.4-2807. The best-fit model is a combination of the thermal emission from the accretion disk and a power-law.[18] The origin of the "soft excess" against the extrapolation of the best-fit model - primarily driven by the counts at the peak of the effective area - is still matter of debate. While this source is known to exhibit a dust scattering halo[18] a contribution from inaccurately calibrated redistribution is still consistent with the data.

tion of the best-fit model in the energy range above the photo-electric cut-off (Fig. 4). Whether this excess is due to inaccurately calibrated redistribution of high energy photons or to emission due to the known scattering halo in this source[18] is still an open issue. This issue can be addressed by simultaneously observing the same source with different instruments (Schultz et al., in preparation).

4 Effective area at energies <10 keV

In optical astronomy, there are many stable point sources (mostly stars) with a range of colors that can be used as standard candles. While there are stable point sources in the at energies lower than 1 keV (e.g., white dwarfs and isolated neutron stars), there are no known stable point sources in

Table 3 Main sources used for the calibration of the effective area below 10 keV

Source	HRC	LETG	HETG	RGS	ACIS	EPIC-MOS	EPIC-pn	GSC	SSC	JEM-X	PCA	XIS	XRT
1E0102-72					X	X						X	X
3C273		X	X										X
Abell1795					X	X	X						X
Abell2029					X	X	X						X
bright Earth limb												X	
Cygnus Loop												X	
Coma cluster						X	X						
Crab Nebula				X				X	X	X	X		X
G21.5-0.9	X				X								X
H1426+428			X										X
HZ43	X	X											
Mkn421	X	X	X	X	X[a]								X
Perseus Cluster						X	X						
PKS2155-304	X	X	X	X	X[a]							X	
RXJ1856.5-3754		X		X								X	X

[a]observations done with a combination gratings+detector.

the medium X-ray band (2–10 keV). For this reason, extended sources (e.g., supernova remnants and clusters of galaxies) are commonly used as standard candles in this band. In addition, only faint point sources can be used to prevent pile-up effects in CCDs, while gratings observations of extended sources are excluded to prevent degradation in the spectral resolution.

4.1 Point-like sources

The most commonly used sources for the in-flight calibration of the soft X-ray effective area are largely coincident with those used for the calibration of the redistribution (Tab. 3). These include compact SNR (1E0102-72.3), active stars with well isolated He-like and H-like emission line complexes (ζPuppis; ζOrionis), and very soft Isolated Neutron Stars (INS; RXJ1856.6-3754). In the EUV/extreme soft X-ray band, White Dwarfs such as Sirius B, GD153 or HZ43 have been used to

create empirical adjustments to the effective area.

In the 2–10 keV band, radio-loud AGN with relative featureless spectra, such as 3C273, H1426+128, and PKS2155-304, are still widely used for effective area calibration. A cross-calibration campaign on PKS2155-304 (now involving *Chandra*, NuSTAR, *Suzaku*, *Swift*, and XMM-Newton) has been running continuously since 2006,[17] with one observation every year. However, radio-loud AGN, and in particular blazars (Mkn421, PKS2155-304) are rapidly variable sources, with complex flux-dependent spectral variability. *Chandra* and XMM-Newton CCD observations of these objects are almost invariably affected by pile-up due to the better spatial resolution of their telescopes, their higher effective area and/or their frame exposure time. For this reason, *Chandra* observes Mkn421 and PKS2155-304 only with the gratings to cut down the flux in the zero-order image. Mitigation actions in grating-less observations (such as those obtained with the EPIC) involve excising the PSF core from the spectral accumulation region, yielding additional uncertainties in the spectral de-convolution due to the possible energy dependence of the Encircled Energy Fraction in the PSF wings.[19] Serendipitous catalogs for effective area calibration and cross-calibration have been alternatively used.[20,21]

Plerionic spectra in Pulsar Wind Nebulae (PWN) may represent a promising alternative (besides the Crab, still used for the calibration of the RXTE/PCA, the NuSTAR instruments, and the instruments on-board MAXI, among others). They are appropriate for calibration purposes thanks to their stability on human time-scales and their simple non-thermal shape (often very well approximated, within the statistical quality of currently available X-ray measurements, by power-laws). The IACHEC study on G21.5-0.9[22] is currently the largest published cross-calibration study ever in terms of number of instruments involved, covering the whole energy band from 2 to 150 keV (the source is obscured by a column density $\simeq 2\times10^{22}$ cm^{-2}). On the other hand, even a compar-

atively compact PWN as G21.5-0.9 ($\sim$3' size, with a central symmetric plerionic core of $\sim$30") may exceed the field-of-view of a narrow field instrument, such as the future high-resolution micro-calorimeter on-board ASTRO-H.

4.2 Molecular contamination

Several missions have discovered after launch a build-up of molecular contamination on cold surfaces within the light path of their instruments.[23,24] This contaminant absorbs X-ray photons at soft energies ($\lesssim$1 keV), and as it builds up the effective area becomes a sensitive but uncertain function of time, location on the detector, and energy.

Measuring and modeling the temporal, spatial, and chemical characteristics of contaminant has proven to be challenging. Regular *Chandra* observations of bright continuum sources such as Mkn 421 with the gratings have been invaluable in measuring absorption edges and constraining the chemical composition of the contaminant on ACIS. Off-axis pointings on Abell 1795 have monitored the spatial dependence (see § 4.3). On the *Suzaku*/XIS, a large amount of contaminant built up very quickly in the first months of the mission, and early and frequent observations of soft, stable sources like 1E0102-72.3 and RXJ1856-6-3754 have been crucial to constrain its on-axis temporal dependence. Observations of the Cygnus Loop and the bright limb of the Earth, which produces field-filling N-K and O-K emission lines, have helped to understand the spatial distribution.

4.3 On galaxy clusters as calibration sources

Galaxy clusters have been extensively used as calibration sources because they are stable on human time-scales. This implies that the sufficiently hot clusters can be used at any time for any hard

X-ray detector calibration observation, and compared with observations taken in other epochs by the same or other detectors. Thus, large cluster samples can be formed for the cross-calibration purposes without the considerable efforts involved in simultaneous cross-mission observation campaigns of variable sources. The largest sample of cross-calibration targets so far is that of the about 50 HIFLUGCS galaxy clusters.[25] The nearest clusters hotter than about 6 keV are bright and hard, thus yielding sufficient photons for calibration experiments within typical standard X-ray calibration experiments' duration (a few hours). However, due to their surface brightness distribution they are not too bright to produce pile-up in CCD detectors. Also, PSF effects can be minimized by extracting data from regions larger than its size. The combination of these factors makes galaxy clusters very suitable targets for effective area shape calibration.

The only significant line emission in clusters hotter than 6 eV is due to recombination transitions from FeXXV and FeXXVI. The energy band covered by these lines ($\simeq$6.67 to 6.96 keV) is narrow. The dependence of the effective area on energy in this energy range is smooth and shallow. This allows decoupling the energy redistribution and effective area calibration effects. However, the extended nature of the X-ray emission in clusters is at the same time a curse and a blessing. It causes different sky areas being covered in different detectors. This requires additional exposure map corrections, known with different degrees of uncertainties in different detectors.

Abell 1795 has been used to monitor the spatial distribution of the contaminant in ACIS. At the same time, galaxy clusters have assumed the role of reference "standard candles" in the 2–10 keV band, following the pioneer cross-calibration work by Nevalainen et al. (2010). These authors found that the gas temperature in clusters of galaxies derived from the 2-6 keV continuum emission is in good agreement with that derived from the H- to He-like Fe line ratio for the EPIC cameras (see, *e.g.*, Fig.10 in Nevalainen et al. 2010). This method requires a very large number of photons

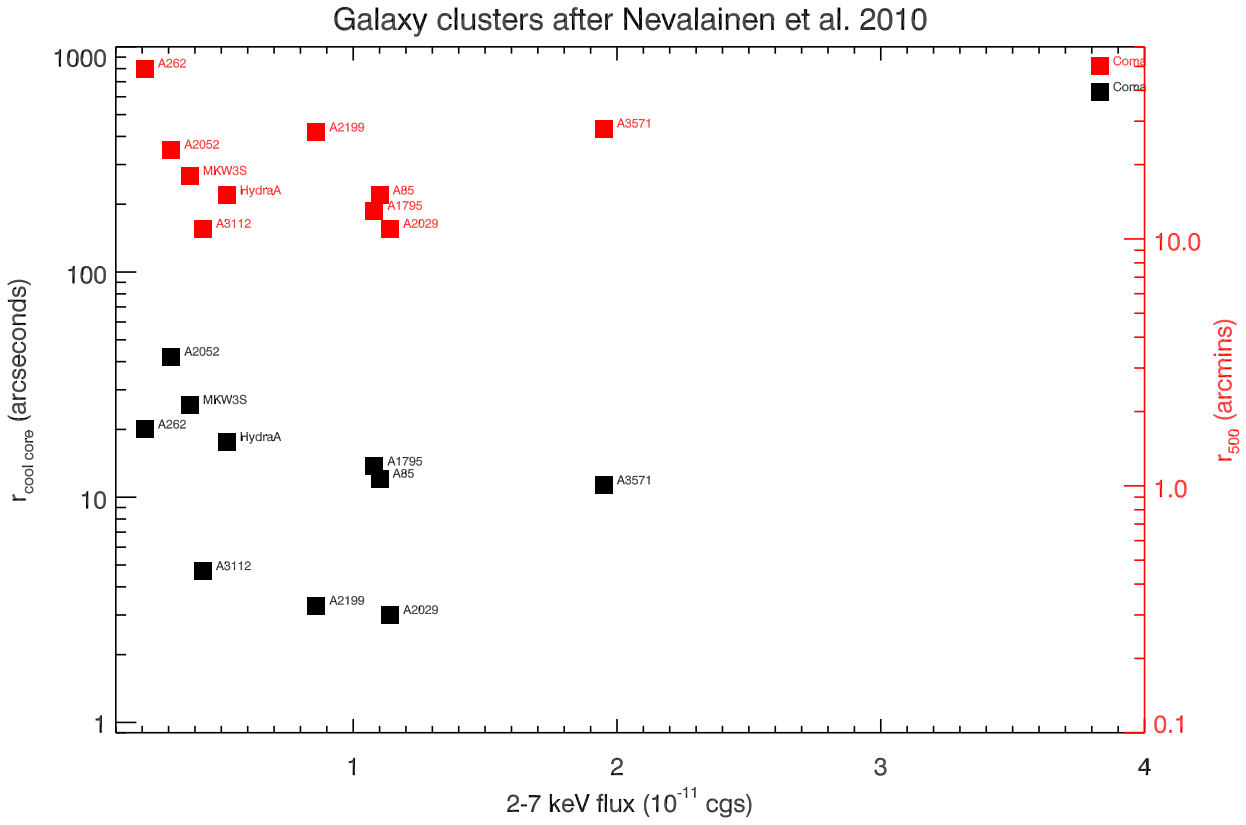

Fig 5 Radius of the cool core ($r_{coolcore}$, *black squares*, *left y-axis*), and r_{500} (*red squares*, *right y-axis*) as a function of the 2–7 keV flux for the sample of galaxy cluster after Nevalainen et al. (2010)

in the narrow range, and has encountered so far limited application with real data, due to the very deep exposures needed. It opens, however, promising perspectives for future high-resolution detectors at the Fe transition energies, such as the micro-calorimeters on board ASTRO-H.

Thanks to their flux stability, and simple, well-understood physics, galaxy clusters are excellent calibrator candidates for the SXS on-board ASTRO-H. The ideal source should have the best combination of X-ray flux, small cool core (in order to ensure the largest possible isothermal area), and extension. These quantities are shown in Fig. 5 for the 11 objects of the Nevalainen et al. (2010) sample (see also Sect. 8).

Table 4 Sources used for the calibration of the effective area above 10 keV

Source	AGILE	BAT	HXD	HEXTE	IBIS	NuSTAR
Crab Nebula	X[a]	X	X	X	X	X
PSR1509-58			X		X	

[a]Crab pulsar

5 Effective area at energies >10 keV

Most of the operational instruments above 10 keV ("hard X-ray band" hereafter) have employed the Crab Nebula as primary calibrator for the effective area. The responses of the INTEGRAL/IBIS, RXTE/PCA[26] and NuSTAR have been calibrated solely based on the Crab, assuming "standard values" for the photon index and normalization of a power-law shape. Weisskopf et al. (2010) showed that some models of the nebula high-energy emission predict a spectral curvature that should be already measurable by the PCA. This evidence challenges the assumption underlying the calibration of its response. The status of the Crab Nebula as "*the* standard candle of X-ray astronomy" has been severely undermined, however, by two circumstances: a) the fact that most instruments operating below 10 keV during the first decade of the XXI century could not observe the Crab due to telemetry or pile-up limits, except in special, rarely used instrumental modes; b) the discovery that the Crab is actually a variable source[27,28] exhibiting variations with a dynamical range of $\simeq$7% over the whole X-ray band on time-scales of months (a discovery delayed by the assumption that the Crab Nebula was a stable calibration source!). Alternative plerionic spectra such as G21.5-0.9[22] and MSH15-52[29,30] could yield a statistical accuracy on the determination of the spectra shape of $\Delta\Gamma\sim$0.05 in a 50 ks observation with the hard X-ray focusing telescopes on NuSTAR and ASTRO-H. With a NuSTAR observation of 280 ks of G21.5-0.9, the error on

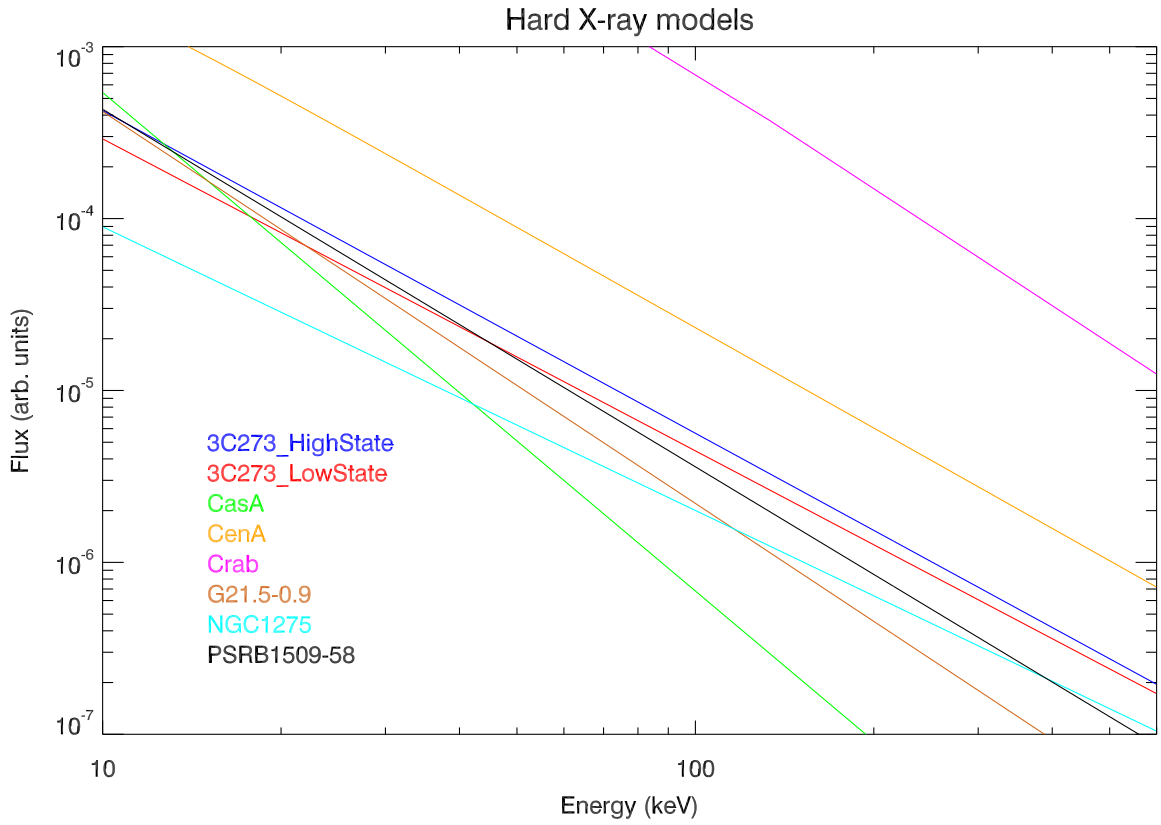

Fig 6 Models of plerionic spectra above 10 keV: Crab (*magenta*);[34] G21.5-0.9 (*brown*);[22] PSR1509-58 (*black*).[30] They are compared to the spectra of the SNR Cas A (*green*),[35] and 3C273 in its lowest (*red*) and highest (*blue*) state in the 2003–2005 INTEGRAL and XMM-Newton monitoring,[36] and NGC 1275 (*cyan*), the AGN at the center of the Perseus Cluster.[37]

the spectral index ($\Delta\Gamma \simeq 0.013$[31]) is comparable to the systematic error due to uncertainties in the effective area calculations (K.Madsen, private communication). Recently, however, an observation by NuSTAR revealed the presence of a break in the spatially integrated spectrum of G21.5-0.9,[31] with the spectral index going from 1.996 to 2.093 across a break at about 9.7 keV. This may eventually explain the systematically higher spectral indexes measured at energies higher than 10 keV.[22] Comparable statistical quality could be obtained on bright radio-loud hard AGN such as 3C273[32] or Centaurus A.[33] However, 3C273 exhibits a hard X-ray flux historical variability of about 50%,[32] and Centaurus A is also a variable source.

In summary, no source is an ideal effective area calibrator in the hard X-ray band. It is recommendable to compile and compare measurements from different sources in order to achieve a good understanding of the hard X-ray effective area (see, *e.g.* the discussion in Madsen et al. (2015),[2] and/or coordinated observations with other observatories to normalize the flux.

Typical observed spectra above 10 keV for the sources discussed in this Section are shown in Fig. 6.

6 PSF

"First-light"-like bright sources such as X-ray binaries (CygX-1, CygX-2, HerX-1), stars (AR Lac, Capella) or bright AGN (3C273, MCG-6-30-15) have been used for this purpose, depending on the brightness limitations. Appropriate sources need to be seen through a low absorbing column density to keep the possible broadening due to Galactic dust scattering[38] to a minimum. The main goal of these calibration experiments is measuring the wings to high precision. Since the contrast of wings to peak can be of several orders of magnitude, one needs many counts to perform such measurements at the required level of accuracy (typically a few percent), even when bright sources are used.

Since significant pile-up is encountered in ACIS observations of bright point sources, the Chandra team has generated a composite on-axis PSF from HRC-I observations of Ar Lac and Capella and an ACIS observation of Her X-1.[39–41] The Ar Lac and Capella data are used to measure the inner and outer core of the on-axis PSF, respectively, while the ACIS observation of Her X-1 (which is heavily piled-up) is used to measure the wings of the PSF. Her X-1 is a bright point source with a low column density and no dust halo. These three observations are re-normalized to produce the on-axis PSF from 0.5" to 10'. Both the on-axis and off-axis PSF are measured and monitored by

yearly HRC-I raster scans of AR Lac.

7 Timing

The preparation of an in-flight timing calibration plan requires observing pulsars and X-ray bursters covering a wide range of periods. This allows covering the different elements contributing to the accuracy of the event time stamping (delays, dead time etc.). At the shortest period range, the Crab pulsar ($\simeq$33 ms) has been the main target used for timing calibration.[42,43] Alternative targets have been: A0535-262 (103 s), AE Aqr (33 s), Am Her (11140 s), Her X-1 (1.237 s), PSR B0540-69 (51 ms) PSR J0537-69 (50 ms), PSR B1055-52 (197 ms), PSR B1509-58 (in MSH15-52; 0.15135 s), and Vela pulsar (88 ms).

8 Cross-calibration

Several IACHEC Working Groups[§] have been engaged in defining "standard candles" for cross-calibration purposes:

- **Clusters of Galaxies**: Nevalainen et al. (2010) discuss a sample of bright clusters of galaxies, used for the verification of the cross-calibration status among the ACIS, the EPIC, and the BeppoSAX/MECS in the 0.7–10 keV energy band. The results of this study stimulated and contributed to the re-calibration of the *Chandra* effective area embedded in the CALDB change between version 3.4 and version 4.1 at the turn of this decade. Later this study was extended to the XIS,[44] contributing to the refinement of the calibration of the time evolution of their contamination layer. More recently this Group has investigated the impact that cross-calibration uncertainties may have on the determination of the galaxy cluster mass

[§] `http://web.mit.edu/iachec/wgs`

and the consequent cosmological parameters through measurements of the intra-cluster gas temperature profile.[25,45]

- **Coordinated observations** (already known as "Effective area"): This WG has been running a cross-calibration campaign on PKS2155-304 since 2006.[17] This campaign comprises simultaneous observations of with *Chandra*, NuSTAR, *Suzaku*, *Swift*, and XMM-Newton (and now NuSTAR). Other blazars such as 3C273 and H1426+428 are the basis of a systematic comparison of the effective area calibration between the *Chandra* gratings and the XMM-Newton X-ray payload (Smith & Marshall, in preparation)

- **Non-thermal SNR**: This WG deals primarily with effective area cross-calibration above 10 keV. This work has assumed additional importance as the pioneer work by Kirsch et al. (2005)[46] on the Crab Nebula, has been later challenged.[28,47] An update of this study, solely based on quasi-simultaneous observations, is being published (Natalucci et al., in preparation). As discussed in § 5 alternative, albeit weaker, plerionic spectra have been proposed for this purpose, such as G21.5-0.9.[22]

- **Thermal SNR**: The compact SNR 1E0102-72.3 has truly become a standard calibration target for redistribution, effective area, and contamination monitoring. A semi-empirical model based on a continuum version of the APEC code[48] was developed to describe its soft X-ray spectrum, and constrained observationally using the RGS spectra. The 1E0102-72.3 spectra are used to constrain the cross-calibration of the effective area at the energy of strong and well-isolated (at CCD resolution) He- and H-like transitions of OVII, OVIII, NeIX, and NeX.[14]

- **White Dwarfs and Isolated Neutron Stars**: The main goal of this WG is the refinement of the LETGS effective area in the softest X-ray energy band (λ>40). Sources used for this purpose are WDs such as GD153, Hz43, and Sirius B, as well as the INS RXJ1856-6-3754.

Fig. 7 represents a synopsis of cross-calibration measurements in the 0.1–10 keV energy band recently as published in IACHEC papers.[14,17,22,44,49] It must be stressed that these results were published at different times, and therefore do *not* correspond to a homogeneous set of calibrations. Readers are warmly encouraged to refer to the continuously updated IACHEC publication web page[¶] for a discussion of the most updated cross-calibration status.

The status of inter-calibration among operational instruments in three energy bands: "soft" (E<2 keV), "medium" ($E\simeq$2–10 keV), and "hard" (E>10 keV) can be summarized as follows:

- **Soft**: energy-dependent cross-calibration discrepancies in this energy band were reported by Nevalainen et al. (2010). Recent results confirm that the ratio between the Chandra/ACIS and XMM-Newton/EPIC-pn fluxes increase from -10% to +10% going from 0.5 to 2 keV (Nevalainen et al., in preparation) . A similar behavior is observed when comparing *Swift*/XRT and XMM-Newton/EPIC-pn. On the other hand, the flux ratio between the Suzaku/XIS and XMM-Newton/EPIC-pn cameras was shown to energy-independent, and comprised between -5% and -10%,[44] although a more recent and extensive study challenges these conclusions (Nevalainen et al., in preparation). XMM-Newton/EPIC-MOS cameras yield fluxes which are on the average in good agreement with EPIC-pn.[21]

- **Medium**: A generally good agreement is shown among all the operational CCD within $\pm$5% in flux and spectral shape[49]

[¶] `http://web.mit.edu/iachec/papers/index.html`

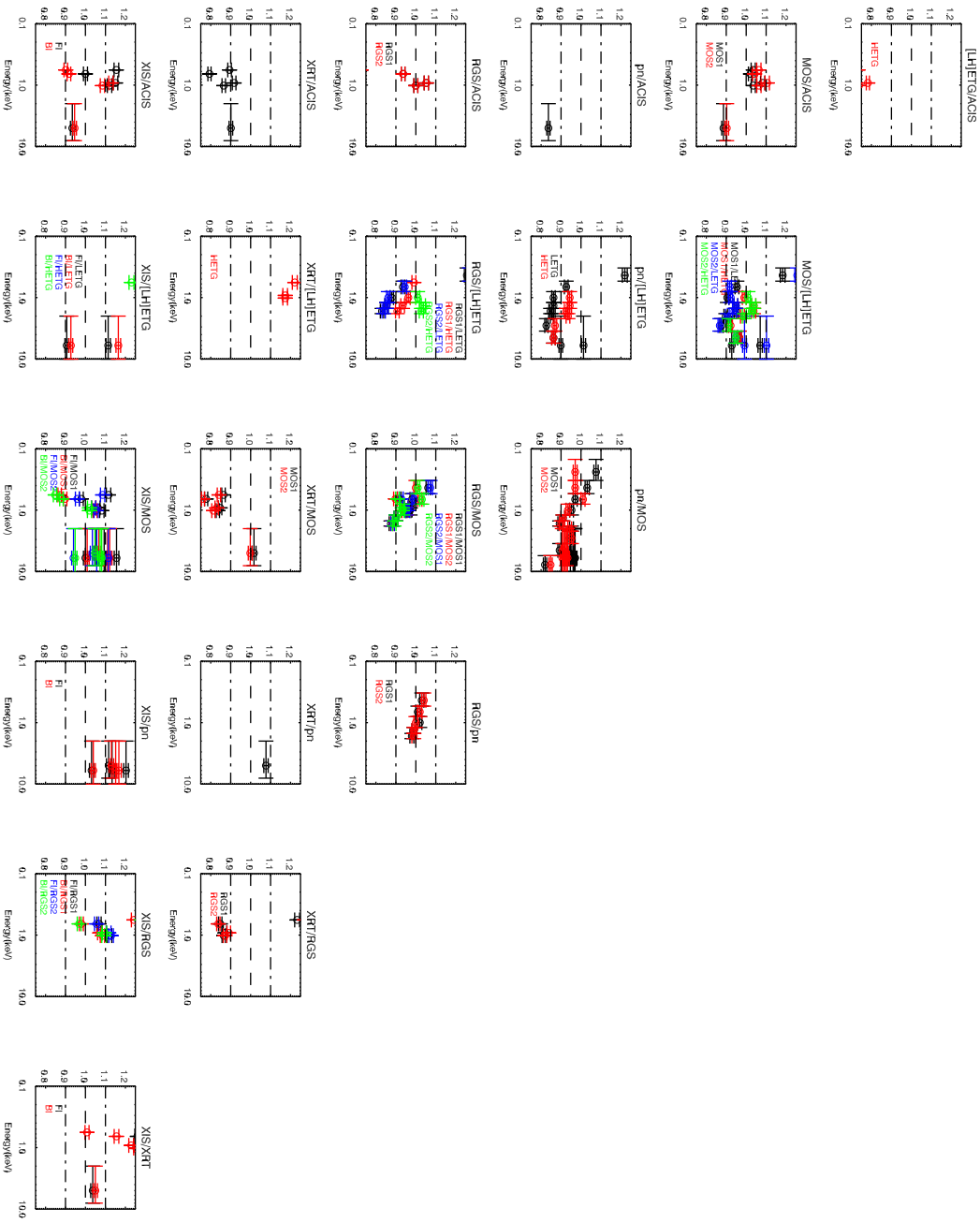

Fig 7 Flux ratios as a function of energy in the 0.1–10 keV energy band for pairs of operational instruments compiled from IACHEC cross-calibration papers published in the last three years.

Table 5 Sources used in IACHEC cross-calibration papers. Legenda: "N10" = Nevalainen et al. 2010; "I11" = Ishida et al. 2011; "T11" = Tsujimoto et al. 2011; "P12" = Plucinsky et al. 2012; "K13" = Kettula et al. 2013. The over 50 galaxy clusters in Schellenberger et al. (2015)[25] are not listed in this Table.

Source	ACIS	EPIC	LETG	ISGRI	MECS	PCA	RGS	XIS	XRT
1E0102-72	P12	P12					P12	P12	P12
Abell 1060		K13						K13	
Abell 1795	N10	N10,K13			N10			K13	
Abell 2029	N10	N10			N10				
Abell 2052	N10	N10			N10				
Abell 2129	N10	N10			N10				
Abell 262	N10	N10			N10				
Abell 3112	N10	N10,K13			N10			K13	
Abell 3571	N10	N10			N10				
Abell 496		K13						K13	
Abell 85	N10	N10			N10				
AWM7		K13						K13	
Centaurus cluster		K13						K13	
Coma cluster	N10	N10,K13			N10			K13	
G21.5-0.9	T11	T11		T11		T11		T11	T11
Hydra A	N10	N10			N10				
MKW3S	N10	N10			N10				
Ophiucus cluster		K13						K13	
PKS2155-304		I11	I11					I11	
Triangulum cluster		K13						K13	

- **Hard**: Swift/BAT yields fluxes $\simeq$20% lower than INTEGRAL/SPI. Spectral indices are in excellent mutual agreement ($\pm$0.04),[22] however. NuSTAR (not operational at the time of the Tsujimoto et al. 2011 paper) also yields fluxes in agreement within a few percent when compared to the *Suzaku*/HXD

Table 5 lists the sources used in IACHEC cross-calibration papers.

9 Summary and conclusions

The main goal of this paper is to describe the variety of celestial sources used to calibrate X-ray space instrumentation. An inevitably sketchy description of the rationale behind their choice over the long history of X-ray astronomy accompanies the enumeration of this variety. While in principle calibration of space instruments should be fundamentally based on a complete physical model of the detector as well as of the collimator or telescope in front of them, various constraints during mission development may impose complementing or verifying the ground-based measurements with observations of celestial sources. The possible degradation of the instrument performance in the harsh space radiation environment may shift further the balance towards the need of a comprehensive set of in-flight calibration observations.

Unfortunately, the X-ray sky does not offer "standard candles" *strictu sensu*, *i.e.* sources whose absolute flux can be accurately estimated once spectral properties can be determined even in non-photometric conditions. For most X-ray sources we must be content with an educated guess of the physical processes responsible for their plasma emission. For this reason, absolute flux calibration is often more challenging than spectral calibration.

X-ray astronomy is a mature science, both scientifically and technologically. Despite more than four decades of science operation of X-ray observatories, however, only very recently has an attempt been initiated to homogenize the definition of in-flight calibration plans, as well as the data reduction and analysis procedures for calibration of X-ray instrumentation. The foundation of the IACHEC has been an instrumental step in this ongoing effort. The scientists gathered in the IACHEC put the experience and know-how consolidated in Tables 1 to 5 at the disposal of the development teams of future X-ray missions. This paper aims at constituting a piece of a collective

heritage on how to optimize in-flight calibration plans.

The scientific payload of each mission is a unique combination. Applying blindly past experience can only yield disaster. However, time in orbit is a precious commodity. If this paper triggers studies and decisions that will permit a more efficient use of the limited time allocated to calibration observations, therefore allowing a mission to produce more and better science for the same budget, it will have reached its primary objective.

Acknowledgments

The IACHEC community is grateful to Marcus Kirsch (European Space Agency) and Steve Sembay (University of Leicester), without whose initiative, impulse and enthusiasm the IACHEC would not exist. Their vision has revolutionized the way calibration of high-energy detectors is being carried out. JN acknowledges a PUT426 grant from the Estonian Research Council.

Appendix A: List of instruments discussed in this paper

- AGILE: Astro-rivelatore Gamma a Immagini LEggero (AGILE)
- BeppoSAX: Medium Energy Concentrator Spectrometer (MECS)
- *Chandra*: Advanced CCD Imaging Spectrometer (ACIS), Low Energy Transmission Grating (LETG), High Energy Transmission Grating (HETG), High Resolution Camera (HRC)
- INTEGRAL: Soft INTEGRAL Gamma-ray Imager (IBIS/ISGRI), Spectrometer on Integral (SPI), Joint European X-ray Monitor (JEM-X)
- MAXI: Gas Slit Camera (GSC), Solid-state Slit Camera (SSC)
- NuSTAR: Nuclear Spectroscopy Telescope ARray (NuSTAR)

- RXTE:High-Energy X-ray Timing Experiment (HEXTE), Proportional Counter Array (PCA)
- *Suzaku*: Hard X-ray Detector (HXD), X-ray Imaging Spectrometer (XIS)
- *Swift*: Burst Alert Telescope (BAT), X-Ray Telescope (XRT)
- XMM-*Newton*: European Photon Imaging Camera (EPIC), Reflection Grating Spectrometer (RGS)

References

1 S. Sembay, M. Guainazzi, P. Plucinsky, and J. Nevalainen, "Defining high-energy calibration standards: IACHEC (International Astronomical Consortium for High-Energy Calibration)," *AIPC* **1248**, 193 (2010).

2 K. Madsen, F. Harrison, C. Markwardt, H. An, B. Grefenstette, M. Bachetti, H. Miyasaka, T. Kitaguchi, V. Bhalerao, F. Christensen, W. Craig, F. Fuerst, D. Walton, C. Hailey, V. Rana, D. Stern, N.-J. Westergaard, and W. Zhang, "Calibration of the NuSTAR High Energy Focusing X-ray Telescope," *ApJ* **in press**, arXiv:1504.01672 (2015).

3 J.-U. Ness, J. Schmitt, V. Burwitz, R. Mewe, A. Raassen, R. van der Meer, P. Predehl, and A. C. Brinkman, "Coronal density diagnostics with Helium-like triplets: CHANDRA-LETGS observations of Algol, Capella, Procyon, epsilon Eri, alpha Cen A&B, UX Ari, AD Leo, YY Gem, and HR 1099," *A&A* **394**, 911 (2002).

4 M. Audard, M. Güdel, J. Drake, and V. Kashyap, "Extreme-ultraviolet flare activity in late-type stars," *ApJ* **541**, 396 (2000).

5 S. S. Lalitha and J. Schmitt, "X-ray activity cycle on the active ultra-fast rotator AB doradus A. implication of correlated coronal and photometric variability," *A&A* **559**, 119 (2013).

6 K. Mitsuda, N. Yamasaki, K. Shinozaki, Y. Takei, T. Nakagawa, H. Sugita, Y. S. R. Fujimoto, T. Ohashi, Y. Ishisaki, Y. Ezoe, M. Murakami, M. Tashiro, Y. Terada, S. S. Kitamoto, T. Tamagawa, M. Kawaharada, T. Mihara, R. Kelley, C. Kilbourne, F. S. Porter, P. Shirron, M. DiPirro, D. McCammon, and J.-W. den Herder, "The x-ray microcalorimeter on the NeXT mission," *SPIE* **7011**, E2KM (2008).

7 L. Barragán, J. Wilms, K. Pottschmidt, M. Nowak, I. Kreykenbohm, R. Walter, and J. Tomsick, "Suzaku observation of IGR J16318-4848," *A&A* **508**, 1275 (2009).

8 F. Fürst, S. Suchy, I.Kreykenbohm, L. Barragán, J. Wilms, K. K. Pottschmidt, I. Caballero, P. Kretschmar, F. C, and R. Rothschild, "Study of the many fluorescent lines and the absorption variability in GX 301-2 with XMM-newton," *A&A* **535**, 9 (2011).

9 J. Torrejón, N. Schulz, M. Nowak, and T. Kallman, "A Chandra survey of fluorescence Fe lines in X-ray binaries at high resolution," *ApJ* **715**, 947 (2010).

10 S. Owocki and D. Cohen, "X-ray line profiles from parameterized emission within an accelerating stellar wind," *ApJ* **559**, 1008 (2001).

11 K. Arnaud, R. Smith, and A. Siemiginowska, *Handbook of X-ray Astronomy*, Cambridge University Press, Cambridge, Mass. (2011).

12 S.Molendi and F.Gastaldello, "Non-thermal emission in the core of Perseus: results from a long XMM-Newton observation," *A&A* **493**, 13 (2009).

13 P. Plucinsky, F. Haberl, D. Dewey, A. Beardmore, J. DePasquale, O. Godet, V. Grinberg, E. Miller, A. Pollock, S. Sembay, and R. Smith, "The SMC SNR 1E0102.2-7219 as a calibration standard for x-ray astronomy in the 0.3-2.5 kev bandpass," *SPIE* **7011**, 2 (2008).

14 P. Plucinsky, A. Beardmore, J. DePasquale, D. Dewey, A. Foster, F. Haberl, E. Miller, A. Pollock, J. Posson-Brown, S. Sembay, and R. Smith, "Cross-calibration of the x-ray instruments onboard the Chandra, Suzaku, Swift, and XMM-Newton observatories using the SNR 1E 0102.2-7219," *SPIE* **8443**, 12 (2012).

15 V. Burwitz, F. Haberl, R. Neuhäuser, P. Predehl, J. Trümper, and V. Zavlin, "The thermal radiation of the isolated neutron star RX J1856.5-3754 observed with Chandra and XMM-Newton," *A&A* **399**, 1109 (2003).

16 N. Sartore, A. Tiengo, S. Mereghetti, A. D. Luca, R. Turolla, and F. Haberl, "Spectral monitoring of RX J1856.5-3754 with XMM-Newton. analysis of EPIC-pn data," *A&A* **541**, 66 (2012).

17 M. Ishida, M. Tsujimoto, T. Kohmura, M. Stuhlinger, M. Smith, H. Marshall, M. Guainazzi, K. Kohei, and T. Ogawa, "Cross spectral calibration of Suzaku, XMM-Newton, and Chandra with PKS 2155-304 as an activity of IACHEC," *PASJ* **63**, 657 (2011).

18 C. Ferrigno, E. Bozzo, M. Falanga, L. Stella, S. Campana, T. Belloni, G. Israel, L. Pavan, E. Kuulkers, and A. Papitto, "INTEGRAL, Swift, and RXTE observations of the 518 Hz accreting transient pulsar Swift J1749.4-2807," *A&A* **525**, 48 (2011).

19 A. Read, S. Rosen, R. Saxton, and J. Ramirez, "A new comprehensive 2d model of the point spread functions of the XMM-Newton EPIC telescopes: spurious source suppression and improved positional accuracy," *A&A* **534**, 34 (2011).

20 S. Mateos, R. Saxton, A. Read, and S.Sembay, "Statistical evaluation of the flux cross-calibration of the XMM-Newton EPIC cameras," *A&A* **496**, 879 (2009).

21 A. Read, M. Guainazzi, and S. Sembay, "Cross-calibration of the XMM-Newton EPIC pn and mos on-axis effective areas using 2XMM sources," *A&A* **564**, 75 (2014).

22 M. Tsujimoto, M. Guainazzi, P. Plucinsky, A. Beardmore, M. Ishida, L. Natalucci, J. Posson-Brown, A. Read, R. Saxton, and N. Shaposhnikov, "Cross-calibration of the X-ray instruments onboard the Chandra, INTEGRAL, RXTE, Suzaku, Swift, and XMM-Newton observatories using G21.5-0.9," *A&A* **525**, 25 (2011).

23 H. Marshall, A. Tennant, C. Grant, A. Hitchcock, S. O. Dell, and P. Plucinsky, "Composition of the Chandra ACIS contaminant," *SPIE* **497**, 5165 (2004).

24 K. Koyama, H. Tsunemi, T. Dotani, M. Bautz, K. Hayashida, T. Tsuru, H. Matsumoto, Y. Ogawara, G. Ricker, J. Doty, S. Kissel, R. Foster, H. Nakajima, H. Yamaguchi, H. Mori, M. Sakano, K. Hamaguchi, M. Nishiuchi, E. Miyata, K. Torii, M. Namiki, S. Katsuda, D. Matsuura, T. Miyauchi, N. Anabuki, N. Tawa, M. Ozaki, H. Murakami, Y. Maeda, Y. Ichikawa, G. Prigozhin, E. Boughan, B. Lamarr, E. Miller, B. Burke, J. Gregory, A. Pillsbury, A. Bamba, J. Hiraga, A. Senda, H. Katayama, S. Kitamoto, M. Tsujimoto, T. Kohmura, Y. Tsuboi, and H. Awaki, "X-Ray Imaging Spectrometer (XIS) on Board Suzaku," *PASJ* **59**, 23 (2007).

25 G. Schellenberger, T. Reiprich, L. Lovisari, J. Nevalainen, and L. David, "Xmm-newton and Chandra cross-calibration using HIFLUGCS galaxy clusters. Systematic temperature differences and cosmological impact," *A&A* **575**, 30 (2015).

26 N. Shaposhnikov, K. Jahoda, C. Markwardt, J. Swank, and T. Strohmayer, "Advances in the RXTE Proportional Counter Array calibration: Nearing the statistical limit," *ApJ* **717**, 59 (2012).

27 C. Greiveldinger and B. Aschenbach, "Temporal Variability of the X-ray Emission of the Crab Nebula Torus," *ApJ* **410**, 305 (1999).

28 C. Wilson-Hodge, M. Cherry, G. Case, W. Baumgartner, E. Beklen, P. N. Bhat, M. Briggs, A. Camero-Arranz, V. Chaplin, V. Connaughton, M. Finger, N. N. Gehrels, J. Greiner, K. Jahoda, P. Jenke, R. Kippen, C. Kouveliotou, H. Krimm, E. Kuulkers, N. Lund, C. Meegan, L. Natalucci, W. Paciesasa, R. Preece, J. Rodi, N. Shaposhnikov, G. Skinner, D. Swartz, A. von Kienlin, R. Diehl, and X.-L. Zhang, "When a standard candle flickers," *ApJ* **727**, 40 (2011).

29 D. Marsden, P. Blanco, D.E., W. Heindl, M. Pelling, L. Peterson, R. Rothschild, A.H.Rots, K. Jahoda, and D. Macomb, "The X-Ray Spectrum of the Plerionic System PSR B1509-58/MSH 15-52," *ApJ* **491**, L39 (1997).

30 T. Mineo, G. Cusumano, M. Maccarone, S. Massaglia, E. Massaro, and E. Trussoni, "The hard x-ray emission from the complex SNR MSH 15-52 observed by BeppoSAX," *A&A* **380**, 695 (2001).

31 M. Nynka, C. Hailey, S. Reynolds, H. An, F. Baganoff, S. Boggs, F. Christensen, W. Craig, E. Gotthelf, B. Grefenstette, F. Harrison, R. Krivonos, K. Madsen, K. Mori, K. Perez, D. Stern, D. Wik, W. Zhang, and A. Zoglauer, "NuSTAR Study of Hard X-Ray Morphology and Spectroscopy of PWN G21.5-0.9," *ApJ* **789**, 72 (2010).

32 S. Soldi, M. Türler, S. Paltani, H. Aller, M. Aller, G. Burki, M. Chernyakova, A. Lähteenmäki, I. McHardy, E. Robson, R. Staubert, M. Tornikoski, R. Walter, and T. J.-L. Courvoisier, "The multiwavelength variability of 3C 273," *A&A* **488**, 411 (2008).

33 Y. Fukazawa, K. Hiragi, S. Yamazaki, M. Mizuno, K. Hayashi, K. Hayashi, S. Nishino,

H. Takahashi, and M. Ohno, "Suzaku view of X-ray spectral variability of the radio galaxy Centaurus A: Partial covering absorber, reflector, and possible jet component," *ApJ* **743**, 124 (2011).

34 T. Kouzu, M. Tashiro, Y. Terada, S. Yamada, A. Bamba, T. Enoto, K. Mori, Y. Fukazawa, and K. Makishima, "Spectral variation of hard X-ray emission from the Crab Nebula with the Suzaku Hard X-ray Detector," *PASJ* **65**, 74 (2013).

35 J. Vink, J. Kaastra, J. Bleeker, and H. Bloemen, "The hard X-ray emission and 44ti emission of Cas A," *AdSpR* **25**, 689 (2000).

36 M. Chernyakova, A. Neronov, T. J.-L. Courvoisier, M. Türler, S. Soldi, V. B. P. Lubiński, R. Walter, K. Page, M. Stuhlinger, R. Staubert, and I. McHardy, "2003-2005 integral and xmm-newton observations of 3c 273," *A&A* **465**, 147 (2007).

37 D. Eckert and S. Paltani, "INTEGRAL observations of the Perseus cluster," *A&A* **495**, 415 (2009).

38 P. Predehl and J. Schmitt, "X-raying the interstellar medium: Rosat observations of dust scattering halos.," *A&A* **293**, 889 (1995).

39 P. Zhao and L. van Speybroeck, "A new method to model x-ray scattering from random rough surfaces," *SPIE* **4851**, 124 (2003).

40 D. Jerius, T. Geatz, and M. Karovska, "Calibration of Chandra's near on-axis optical performance," *SPIE* **5165**, 433 (2004).

41 T. Gaetz, R. Edgar, D. Jerius, P. Zhao, and R. Smith, "Calibrating the wings of the chandra PSF," *SPIE* **5165**, 411 (2004).

42 Y. Terada, T. Enoto, R. Miyawaki, Y. Ishisaki, T. Dotani, K. Ebisawa, M. Ozaki, Y. Ueda, L. Kuiper, M. Endo, Y. Fukazawa, T. Kamae, M. Kawaharada, M. Kokubun, Y. Kuroda, K. Makishima, K. Masukawa, T. Mizuno, T. Murakami, K. Nakazawa, A. Nakajima, M. Nomach, N. Shibayama, T. Takahashi, H. Takahashi, M. Tashiro, T. Tamagawa, S. Watanabe, M. Yamaguchi, K. Yamaoka, and D. Yonetoku, "In-orbit timing calibration of the Hard X-ray Detector on board Suzaku," *PASJ* **60**, 25 (2008).

43 A. Martin-Carrillo, M. Kirsch, I. Caballero, M. Freyberg, A. Ibarra, E. Kendziorra, U. Lammers, K. Mukerjee, G. Schönherr, M. Stuhlinger, R. Saxton, R. Staubert, S. Suchy, A. Wellbrock, N. Webb, and M. Guainazzi, "The relative and absolute timing accuracy of the EPIC-pn camera on XMM-Newton, from X-ray pulsations of the Crab and other pulsars," *A&A* **545**, 146 (2012).

44 K. Kettula, J. Nevalainen, and E. Miller, "Cross-calibration of Suzaku/XIS and XMM-Newton/EPIC using galaxy clusters," *A&A* **552**, 47 (2013).

45 H. Israel, G. Schellenberger, J. Nevalainen, R. Massey, and T. Reiprich, "Reconciling Planck cluster counts and cosmology? Chandra/XMM instrumental calibration and hydrostatic mass bias," *MNRAS* **448**, 814 (2015).

46 M. Kirsch, U. Briel, D. Burrows, S. Campana, G. Cusumano, K. Ebisawa, M. Freyberg, M. Guainazzi, F. Haberl, K. Jahoda, J. Kaastra, P. Kretschmar, S. Larsson, P. L. K. Mori, P. Plucinsky, A. Pollock, R. Rothschild, S. Sembay, J.Wilms, and M. Yamamoto, "Crab: the standard x-ray candle with all (modern) x-ray satellites," *SPIE* **5898**, 22 (2005).

47 M. Weisskopf, M. Guainazzi, K. Jahoda, N. Shaposhnikov, S. O'Della, V. Zavlin, C. Wilson-

Hodge, and R. Elsner, "On calibrations using the Crab Nebula and models of the nebular X-ray emission," *ApJ* **713**, 912 (2010).

48 A. Foster, L. Ji, R. K. R.K. Smith, and N. Brickhouse, "Updated atomic data and calculations for x-ray spectroscopy," *ApJ* **758**, 128 (2012).

49 J. Nevalainen, J. David, and M. Guainazzi, "Cross-calibrating X-ray detectors with clusters of galaxies: an IACHEC study," *A&A* **523**, 22 (2010).